Correspondence to:
F. Duru,
firdevs-duru@uiowa.edu

Dayside episodic ion outflow from Martian magnetic cusps and/or magnetosheath boundary motion associated with plasma oscillations

F. Duru[1], D. A. Gurnett[1], D. D. Morgan[1], R. Lundin[2], I. H. Duru[3,4], J. D. Winningham[5], and R. A. Frahm[5]

[1]Department of Physics and Astronomy, University of Iowa, Iowa City, Iowa, USA, [2]Swedish Institute of Space Physics, Kiruna, Sweden, [3]Department of Mathematics, Izmir Institute of Technology, Izmir, Turkey, [4]Science Academy, Istanbul, Turkey, [5]Southwest Research Institute, San Antonio, Texas, USA

Abstract The radar sounder on the Mars Express Spacecraft is able to make measurements of electron densities in the Martian ionosphere from both local electron plasma oscillations and remote soundings. A study of thousands of orbits shows that in some cases the electron plasma oscillations disappear and reappear abruptly near the upper boundary of the dayside ionosphere. In some cases, the Analyzer of Space Plasmas and Energetic Atoms (ASPERA-3) data show clear evidence of upwardly accelerated ionospheric ions, on interconnected magnetic field lines. In other cases, ASPERA-3 data show that when the plasma oscillations disappear, the spacecraft is in the magnetosheath and when they return, the ionospheric plasma reappears. These intermittent appearances of plasma suggest the multiple crossings of the magnetosheath boundary. The motion of the boundary or plasma clouds and ionospheric streamers (a relatively narrow strip of plasma attached to the ionosphere) can cause these multiple crossings.

1. Introduction

The radar sounder MARSIS (Mars Advanced Radar for Subsurface and Ionospheric Sounding) [*Picardi et al.*, 2004] on board Mars Express Spacecraft (MEX) [*Chicarro et al.*, 2004] provides local ionospheric electron densities by means of the detection of local plasma oscillations, as well as the remote sounding of the ionosphere. A study of thousands of local electron density profiles shows that in some cases the electron plasma oscillations disappear and then reappear abruptly on the dayside ionosphere. This paper studies these cases and explores possibilities which could cause these time variations with the help of the Analyzer of Space Plasmas and Energetic Atoms (ASPERA-3) electron spectrometer (ELS) and ion mass analyzer (IMA) data. There are three possible reasons for these variations: (1) plasma outflow at Martian magnetic cusps, (2) oscillation of the ionosphere-magnetosphere boundary, and (3) a detached cloud or elongations of the ionosphere by the solar wind, or a bubble of sheath plasma.

MARSIS, which is a low-frequency radar sounder designed to perform subsurface and ionospheric sounding, consists of a 40 m tip-to-tip dipole antenna, a radio transmitter, and a digital signal processing system [*Picardi et al.*, 2004; *Jordan et al.*, 2009]. The first results of the remote sounding with MARSIS were presented by *Gurnett et al.* [2005]. Remote sounding is performed by sending a short radio pulse of a given frequency f and then measuring the time delay of the returning echo. In the simplest case, waves that are incident normal to a reflective surface are reflected back to the sounder, at the altitude where the wave frequency is equal to the electron plasma frequency.

In addition to remote radio sounding, local electron plasma oscillations excited by the radar transmitter provides a method of measuring the electron density at the position of the spacecraft. As the transmitter steps in frequency, strong local electrostatic plasma oscillations are excited when the wave frequency is equal to the local electron plasma frequency. The electron plasma oscillations are usually very intense and with the antenna voltages being much greater than the dynamic range of the preamplifier-receiver system, the received waveforms are often severely clipped. The resulting distortion causes harmonics of the electron plasma frequency (f_p) to appear in the receiver, which are seen as equally spaced vertical lines on the upper left corners of the ionograms (see Figure F2 from *Duru et al.* [2008]). From the frequency of the oscillation, the local electron density (n_e) can then be calculated using the formula $f_p = 8980 \sqrt{n_e}$, where f_p is in Hertz and n_e is in cm^{-3} [*Gurnett and Bhattacharjee*, 2005]. For more information on how the local electron densities are obtained with MARSIS, see *Duru et al.* [2008].
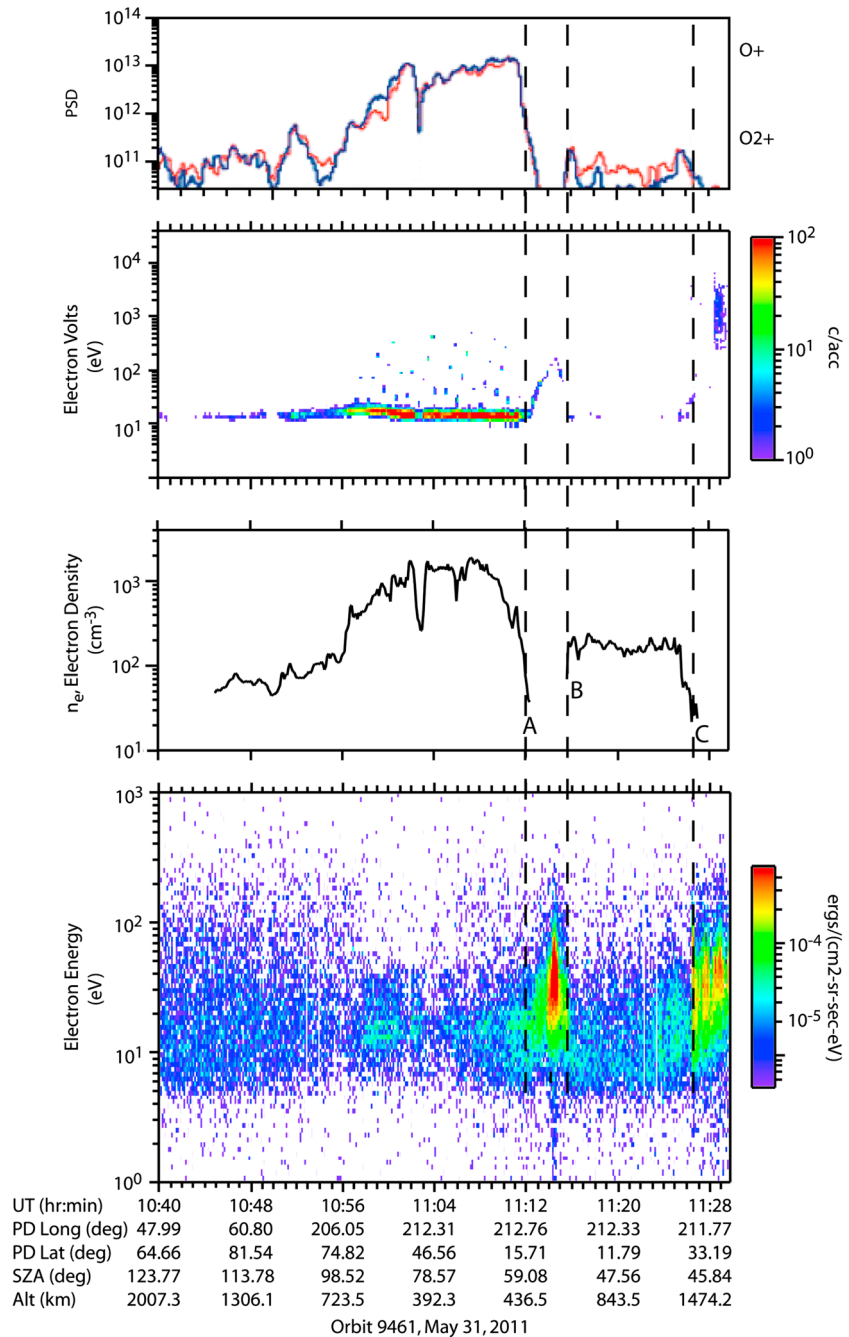
Figure 1. MARSIS and ASPERA-3 data for the pass on 31 May 2011. (fourth row) Color code shows the electron energy flux, at each energy, from ASPERA-3 ELS and (third row) solid black line displays local electron number density values from MARSIS. (second row) The ion count from ASPERA-3 IMA, at each energy. (first row) The phase-space density (PSD) of O^+ and O^{2+} obtained by ASPERA-3.

ASPERA-3 data are used to further investigate the observations made with MARSIS. ASPERA-3, which is designed to study the plasma and neutral gas environment in near-Mars space, consists of an electron spectrometer (ELS), an ion mass analyzer (IMA), a neutral particle imager, a neutral particle detector, a scanner, and a digital processing unit [*Barabash et al.*, 2004]. The ELS is an ultralight, low-power spherical top hat sensor, which measures electrons with energies from 0.4 eV/q to 20 keV/q [*Frahm et al.*, 2006]. The IMA consists of an elevation analyzer, electrostatic top hat, and an orange section style magnetic velocity filter. The elevation analyzer provides the view of up to $\pm 45°$ in 16 steps of elevation or roughly

every 5 to 6°. The electrostatic top hat deflection allows a 360° view in 16 segments, i.e., every 22.5° of azimuth. The orange section style of magnetic filter provides momentum analysis allowing a mass spectrum up to about 40 amu to be determined [*Barabash et al.*, 2006].

2. Description of the Data

A pass with disappearing and reappearing local electron plasma oscillations is shown in Figure 1 (orbit 9461). In this figure, the MARSIS local electron densities are given by the black solid line (third row). The color code in the fourth row (second row) provides electron (ion) flux from ASPERA-3 ELS (IMA) at each energy. Figure 1 (first row) shows the phase-space density (PSD) of the O^+ (red line) and O^{2+} (blue line). In this pass from 31 May 2011, the spacecraft approaches Mars periapsis from the nightside. Low-energy ionospheric ions are observed at the beginning of the pass. Between about 10:58 UT and 11:06 UT, a minor solar wind halo/strahl component of the electrons, given by the violet region at about 100 eV, disappears and ionospheric photoelectron plasma is observed. The halo/strahl electrons are used to identify the extent of penetration of solar wind into the Martian ionosphere [*Dubinin et al.*, 1994]. Simultaneously, we observe an order of magnitude decrease of the O^+ and O2+ PSD. All of this indicates that 11:03 UT is the time of episodic entry into the magnetosheath boundary, where a drop both in PSD and local electron density is observed. At about 11:06 UT, periapsis is reached, where the MARSIS local density and the O^+/O^{2+} PSD approach their maximum values. Notice the general agreement between the ion PSD and the MARSIS density variability near pericenter. The electron flux starts to increase at around 11:09 UT. At about 11:12 UT (point A), ELS begins to observe low-energy magnetosheath plasma. Around the same time, both the MARSIS density and the O^+/O^{2+} PSD drops below threshold (point A). The MARSIS density and O^+/O^{2+} PSD returns back to detectable levels again around 11:16 UT (point B). Between these times, accelerated heavy ions-ion flux shows an arch-like structure and electron magnetosheath fluxes are observed. After 11:16 UT, ELS shows similar structure (strahl electrons) as before the sheath plasma is encountered, while the ion and MARSIS panels indicate the reappearance of ionospheric ion, now stagnant and depleted in density. MARSIS and ionospheric ion densities go below the measurement threshold around 11:27 UT (point C) for the remainder of the pass. The electron and solar wind H^+ signature of full magnetosheath entry appears at around the same time. Between point C and the entrance to sheathlike electrons IMA low-energy ions exhibit a partial arch similar to the earlier one between A and B. This kind of behavior of the ASPERA-3 data is observed in every case, suggesting the multiple crossings of the boundary.

However, in some cases such as the one described above, a more detailed study of the ASPERA-3 data reveals upward acceleration of ions between point A and B. In such a case, ASPERA-3 IMA data, thanks to their mass separation capability, imply a 100 V acceleration of ionospheric O^{2+} ions. However, there is no clear evidence of downward accelerating electrons. Comparisons of electron phase space distributions between points A and B are similar to those found in the sheath.

3. Discussion

The energy flux displayed in Figure 1 would suggest that magnetosheath plasma is detected (the electron fluxes are more than 2 times higher in the magnetosheath than in the ionosphere) whenever the electron plasma oscillation harmonics are lost, implying that the spacecraft crosses the boundary between the ionosphere and magnetosheath several times. However, further investigation of the ASPERA-3 data reveals that in some cases these interruptions in the MARSIS local density data are associated with upward acceleration of the ions. Although the upward motion of the ions is clear in the ASPERA-3 data, the possibility of downward acceleration of the electrons remains unclear. The electron data show distributions similar to those found later in the sheath which could indicate no acceleration. If there were a clear evidence of downward accelerating electrons in addition to the upward moving ions, our conclusion would have been an auroral cavity [*Benson and Cavert*, 1979; *Calvert*, 1981]. Decrease in the ionospheric density at the regions of auroral ion plasma acceleration is discussed by many previous studies [*Lundin et al.*, 1994; *Lundin et al.*, 2006a, 2006b]. However, our data present a region of depleted local electron density, where it is suggested—since there is no magnetometer on board, no definite statement can be made on the magnetic field structure—that MEX is traversing magnetic field lines connected to a "crustal magnetic field cusp" with ion acceleration, but no clear evidence of electron acceleration. Therefore, we can only
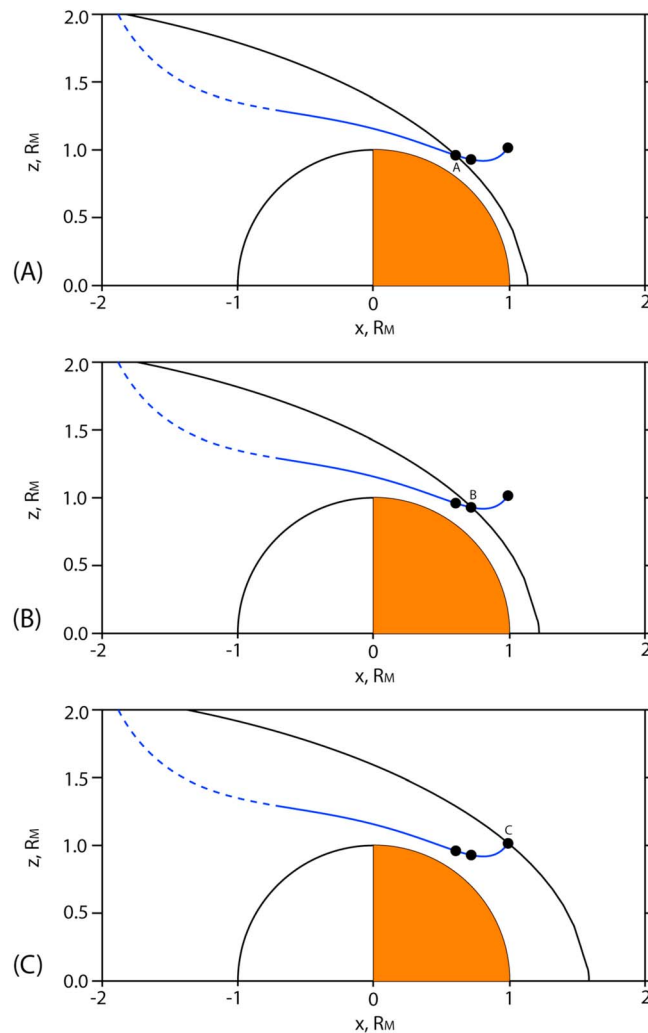
Figure 2. The sequence of three figures shows how multiple crossings are produced by the motion of the ionosphere-magnetosheath boundary. The plots are in cylindrical coordinates. The Sun-Mars direction is given on *x* axis and *y* axis and shows the cylindrical radius. In these three panels, the black and blue lines are the ionosphere-magnetosheath boundary and the trajectory of MEX, respectively. The spacecraft moves from left to right, whereas the boundary oscillates up and down. (a) MEX exits the ionosphere for the first time. (b) Ionosphere, moving outward, catches up to MEX. (c) MEX exits the ionosphere for the last time.

speculate on the process that leads to the ionospheric plasma density cavity. One possibility is that the ions are heated by waves in a transverse acceleration. Another is that field-aligned wave ponderimotive forcing accelerates ions upward along interconnected magnetic field lines.

In order to investigate the parameters and conditions of the possible multiple boundary crossings, we chose the most obvious cases of the disappearance and reappearance of the local plasma oscillations. The observed cases are on the dayside, in the solar zenith angle range between 39° and 58°. In each case, the first crossing is very close to the average predicted location of the boundary altitude.

A boundary oscillation, possibly in response to disturbances in the solar wind, could cause these multiple boundary crossings. Figure 2 shows how the three crossings would be obtained as the boundary oscillates. The solid black line is the boundary between the ionosphere and shocked solar wind, and the blue line shows the trajectory of MARSIS for the pass in Figure 1. After the periapsis, spacecraft altitude increases for the remainder of the pass. When it comes to the point labeled by A in Figure 1, the boundary and the spacecraft coincide for a first brief time period (Figure 2a). Then, the spacecraft leaves the ionosphere. After this point the boundary moves closer to Mars for a while and then reverses direction and moves away from

Table 1. Periods of Oscillations and Boundary Velocity Amplitudes in the Case of a Moving Boundary and the Size of the Cloud Along MEX Trajectory in the Case of a Plasma Cloud

Orbit #	Date	Period of Oscillations	Boundary Velocity Amplitude	Size of the Plasma Cloud Along MEX Trajectory
9461	31 May 2011	6.37 min	16.25 km/s	2776 km
9507	13 June 2011	8.25 min	12.27 km/s	544 km
9553	27 June 2011	8.65 min	5.34 km/s	484 km

Mars. At point B on Figure 1, the boundary catches up to the spacecraft as shown in Figure 2b. For a while the boundary continues to move away from Mars and then reverses direction to approach Mars. During this time, the spacecraft is in the ionosphere. The boundary and MEX meet again, for the last time during this pass, at point C of Figure 1 (Figure 2c). The simplest assumption would be that the boundary oscillates radially in a quasi-sinusoidal manner. This could be either due to a wave, a corrugated boundary, a cusp-like feature, or a quasi-static response to solar wind pressure variations. Unfortunately, with these data it is not possible to distinguish between these possible cases. In the boundary oscillation equations below, the altitude of the boundary at any time t is given by $h(t)$. Here $h0$ is the equilibrium point (average altitude of the boundary), A is the amplitude, ω is the angular velocity, ϕ is the phase shift of the zero offset, and $V(t)$ is the velocity of the boundary at any time. The maximum velocity (V_{max}) is given by $A\,\omega$.

$$h(t) - h0 = A\cos(\omega t + \varphi) \tag{1}$$

$$V(t) = -A\,\omega\sin(\omega t + \varphi) \tag{2}$$

$$V_{max} = |A\,\omega| \tag{3}$$

By solving the above equations using the three crossing points, we were able to obtain oscillation periods and maximum velocity, for the three passes, which provided the best cases of disappearing and reappearing plasma oscillations (summarized in Table 1). To achieve this, an assumption is made for the altitude of the equilibrium point. For the solar zenith angle range determined at the crossings, around 40°, 500 km is a good assumption for the altitude of the boundary. For $h0 = 500$ km, the periods are found to be 8.65, 6.37, and 8.25 min, and the amplitudes of the boundary velocity are 5.34, 16.23, and 12.27 km/s, respectively, for three examples of passes through the dayside. The boundary velocities computed with this analysis are greater than the velocity of the spacecraft for the three example passes, which is between 3.8 and 4.2 km/s. The maximum boundary speeds must be greater than that of the spacecraft so that the boundary can catch the MEX spacecraft after their first encounter.

The motion of the ionospheric boundary, its speed and period, has been studied extensively for the Earth. *Kaufmann and Konradi* [1973] concluded that the velocity of the magnetopause always remains below 20 km/s. The boundary oscillating in a sinusoidal manner is the most common assumption used to calculate the speed of the boundary using a single satellite [*Kaufman and Konradi*, 1969]. Dayside magnetopause crossings showed that the boundary oscillates with a period of about 10 min. [*Kaufmann and Konradi*, 1973]. *Aubry et al.* [1971] used the multiple crossings of the OGO 5 satellite with the magnetopause to deduce that the magnetopause motion is composed of large oscillations, with periods between 3.5 to 6 min and small oscillations with periods around 10 s. The findings of our study, which estimate periods around 7 min for Mars, are comparable to large period oscillations from *Aubry et al.* [1971] for Earth.

An alternative explanation could be that MEX encounters plasma clouds or long streamers attached to the ionosphere, producing multiple crossings of the boundary. Mars' ionosphere is almost certainly not axisymmetric and smooth. Also, clouds of plasma above the ionopause or elongations of the ionosphere into the solar wind are often encountered at Venus [*Brace et al.*, 1982], within the ionosheath. Although the actual process which may form these clouds or streamers is not known, it is suggested that they may be a result of Kelvin-Helmholtz instability. *Tereda et al.* [2002] provides extensive hybrid simulations on Venus, showing that Kelvin-Helmholtz instability can easily be responsible for events like the one in question to happen around the boundary region. The Kelvin-Helmholtz waves have small amplitudes at the beginning, grow, and form votices. These vortex structures may detach and form ionospheric clouds or stay attached to the ionosphere [*Brace et al.*, 1982]. A sketch showing how Kelvin-Helmholtz instabilities might develop around
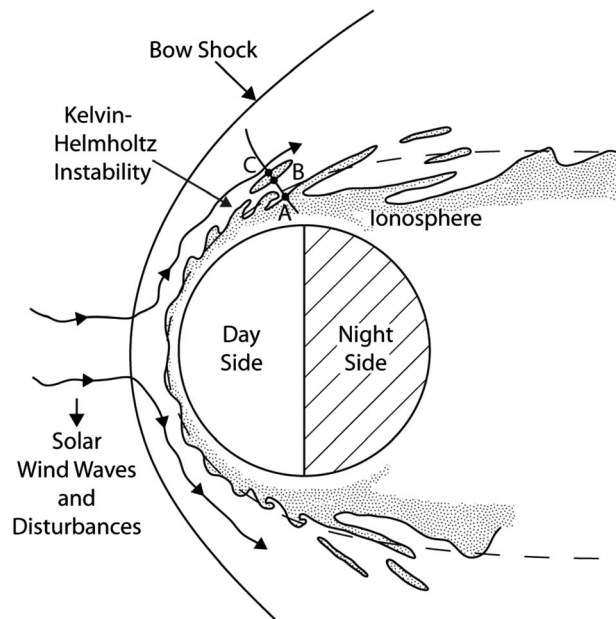
Figure 3. The plasma environment of Mars, with an emphasis on the Kelvin-Helmholtz instabilities and plasma clouds. MEX exits the ionosphere (A). MEX enters a plasma cloud (B). MEX exits a plasma cloud (C).

Mars is given by Figure 3. The outer solid black line is the bow shock, and the dashed line shows the boundary between the ionosphere and the magnetosheath. As can be seen in the figure, instabilities cause turbulence around the boundary, leading to long streamers or plasma clouds. These structures can produce multiple crossings of the boundary. For an example of an isolated cloud of ionospheric plasma, the spacecraft which enters the magnetosheath from ionosphere (point A) would travel for some time in the magnetosheath. Then, it would enter the ionopheric elongation or cloud (point B) and exit it again (point C) for the last time. Between A and B, and after C, magnetosheath plasma would be observed. Between B and C, ionospheric plasma would be detected by the spacecraft. According to the cases studied, if the multiple crossings are due to these clouds or streamers, they should be large structures with sizes along the trajectory of the spacecraft are 2776 km, 544 km, and 484 km. Since the Kelvin-Helmholtz instability tends to cause vortices mostly near the terminator, it is unlikely to be the cause of the observed crossings on the dayside; however, it remains a possibility and cannot be ruled out as a cause.

4. Summary

Investigation of thousands of MEX orbits revealed that in a few passes, the local electron plasma density data disappear and reappear again over intervals of approximately 10 min. The reason for this behavior is the ion outflow from the magnetic cusp regions in some of the cases, where upward accelerating ions can be seen clearly in the ASPERA-3 data. In other cases, it is not clear if the "density holes" are associated with this phenomenon or if they are due to the spacecraft's crossing the boundary between the ionosphere and magnetosheath several times during a given pass.

Assuming multiple crossings of the boundary, the clearest three cases are used to understand the possible motion of the boundary between the magnetosheath and ionosphere. The assumption of a boundary oscillating in a sinusoidal manner is used, and an assumption for the equilibrium point of oscillations is made. The periods of oscillations for the three cases are found to be 8.65, 6.37, and 8.25 min, which is comparable to the period of large amplitude fluctuations calculated for Earth's magnetopause. Existence of plasma clouds or ionospheric streamers due to some instabilities could be another reason for the multiple crossings. In that case, the clouds should be structures with dimensions larger than 500 km along the trajectory of the spacecraft. All the results are summarized on Table 1.

With the information in hand, it is not possible to know if the multiple crossings are due to oscillating boundary, plasma clouds, cusp geometry, some stationary waves, or another reason affecting the ionosphere-magnetosheath boundary.

References

Aubry, M. P., M. G. Kivelson, and C. T. Russell (1971), Motion and the structure of the magnetopause, *J. Geophys. Res.*, *76*(7), 1673–1696.
Barabash, S., et al. (2004), ASPERA-3 analyzer of space plasmas and energetic atoms, Mars Express: The Scientific Payload, European Space Agency Special Report SP-1240, European Space Agency Research and Scientific Support, European Space Research and Technology Centre, Noordwijk, The Netherlands, p. 121.

Barabash, S., et al. (2006), The analyzer of space plasmas end energetic atoms (ASPERA-3) for the Mars Express mission, *Space Sci. Rev.*, *126*(1–4), 113–164, doi:10.1007/s11214-006-9124-8.

Benson, R. F., and W. Cavert (1979), ISIS 1 observations at the source of auroral kilometric radiation, *Geophys. Res. Lett.*, *6*(6), 479–482.

Brace, L. H., R. F. Theis, and W. R. Hoegy (1982), Plasma clouds above the ionopause of Venus and their implications, *Planet. Space Sci.*, *30*(1), 29–37.

Calvert, W. (1981), The auroral plasma cavity, *Geophys. Res. Lett.*, *8*(8), 919–921.

Chicarro, A., P. Martin, and R. Traunter (2004), Mars Express: A European mission to the red planet, in *MARS EXPRESS. The Scientific Payload, SP-1240*, edited by A. Wilson, pp. 3–16, ESA Publication Division, Noordwijk, Netherlands.

Dubinin, E., R. Lundin, and K. Schwingenschuh (1994), Solar wind electrons as tracers of the Martian magnetotail topology, *J. Geophys. Res.*, *99*(A11), 21,233–21,240.

Duru, F., D. A. Gurnett, D. D. Morgan, R. Modolo, A. Nagy, and D. Najib (2008), Electron densities in the upper ionosphere of Mars from the excitation of electron plasma oscillations, *J. Geophys. Res.*, *113*, A07302, doi:10.1029/2008JA013073.

Frahm, R. A., et al. (2006), Location of atmospheric photoelectron energy peaks within the Mars environment, *Space Sci. Rev.*, *126*, 389.

Gurnett, D. A., and A. Bhattacharjee (2005), *Introduction to Plasma Physics With Space and Laboratory Application*, pp. 91, Cambridge Univ. Press, Cambridge, U. K.

Gurnett, D. A., et al. (2005), Radar soundings of the ionosphere of Mars, *Science*, *310*, 1929–1933.

Jordan, R., et al. (2009), The Mars Express MARSIS sounder instrument, *Planet. Space Sci.*, *57*, 1975–1986.

Kaufman, R. L., and A. Konradi (1969), Explorer 12 magnetopause observations: Large-scale nonuniform motion, *J. Geophys. Res.*, *74*(14), 3609–3627.

Kaufmann, R. L., and A. Konradi (1973), Speed and thickness of the magnetopause, *J. Geophys. Res.*, *78*(28), 6549–6568.

Lundin, R., L. Eliasson, G. Haerendel, M. Boehm, and B. Holback (1994), Large-scale auroral plasma density cavities observed by Freja, *Geophys. Res. Lett.*, *21*(17), 1903–1906.

Lundin, R., et al. (2006a), Plasma acceleration above Martian magnetic anomalies, *Science*, *311*, 980–985.

Lundin, R., D. Winningham, S. Barabash, and the Analyzer of Space Plasmas and Energetic Atoms 3 team (2006b), Ionospheric plasma acceleration at Mars: ASPERA-3 results, *Icarus*, *182*(2), 308–319.

Picardi, G., et al. (2004), *Mars Express: A European Mission to the Red Planet, SP-1240*, pp. 51–70, ESA Publication Division, Noordwijk, Netherlands.

Tereda, N., S. Machida, and H. Shinagawa (2002), Global hybrid simulation of the Kelvin-Helmholtz instability at the Venus ionopause, *J. Geophys. Res.*, *107*(A12), 1471, doi:10.1029/2001JA009224.